Planar auxeticity from various inclusions

Artur A. Poźniak[1]
Krzysztof W. Wojciechowski[2]
Joseph N. Grima[3]
Luke Mizzi[4]

[1]Institute of Physics, Poznań Universty of Technology, Piotrowo 3, 60-695 Poznań [2]Institute of Molecular Physics PAS, M. Smoluchowskiego 17, 60-179 Poznań [3]Department of Chemistry, Faculty of Science, University of Malta, Msida, MSD 2080 [4]Metamaterials Unit, Faculty of Science, University of Malta, Msida, MSD 2080

15th September 2015

AUXETICS 2015

Motivation

What is an **auxetic**?

$\nu < 0$ (**N**egtative **P**oisson's **R**atio) is for mechanics what negative refractive index is for optics $n < 0$.
Auxetics are metamaterials.

Beneficial features from NPR

Resistance to shape change and indentation; crack resistance; better vibration absorption (including acoustic one); synclastic curvature, different dynamics.

Applications of NPR materials

Medicine (stents, bandages, implants), defence (energy absorption), furniture industry (better mattresses $\rightarrow$ indentation), automotive industry and sports (safety belts).

Poisson's ratio (stretching along x axis)

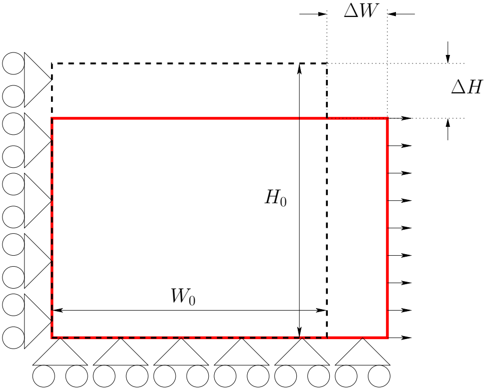

Formal definition

$$\nu_{xy} = -\frac{\epsilon_{yy}}{\epsilon_{xx}} = \frac{s_{yyxx}}{s_{xxxx}}$$

Engineering definition

$$\nu = -\frac{\dfrac{\Delta H}{H_0}}{\dfrac{\Delta W}{W_0}}$$

Motivation – rotating units

Grima, J. N., Alderson, A., & Evans, K. E. (2005). Auxetic behaviour from **rotating rigid** units. Physica Status Solidi (B), 242(3), 561–575.

Grima, J. N., Chetcuti, E., Manicaro, E., Attard, D., Camilleri, M., Gatt, R., & Evans, K. E. (2011). On the auxetic properties of generic **rotating rigid triangles**. Proceedings of the Royal Society A: Mathematical, Physical and Engineering Sciences, 468(2139), 810–830.

Grima, J., Zammit, V., Gatt, R., Alderson, A., & Evans, K. (2007). Auxetic behaviour from rotating **semi-rigid units**. Physica Status Solidi (B), 244(3), 866–882.

Motivation – rotating units

Grima, J. N., Alderson, A., & Evans, K. E. (2005). Auxetic behaviour from **rotating rigid** units. Physica Status Solidi (B), 242(3), 561–575.

Grima, J. N., Chetcuti, E., Manicaro, E., Attard, D., Camilleri, M., Gatt, R., & Evans, K. E. (2011). On the auxetic properties of generic **rotating rigid triangles**. Proceedings of the Royal Society A: Mathematical, Physical and Engineering Sciences, 468(2139), 810–830.

Grima, J., Zammit, V., Gatt, R., Alderson, A., & Evans, K. (2007). Auxetic behaviour from rotating **semi-rigid units**. Physica Status Solidi (B), 244(3), 866–882.

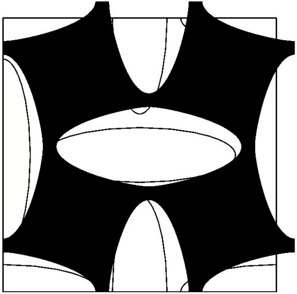

Our result from 2010

Motivation – rotating units

Grima, J. N., Alderson, A., & Evans, K. E. (2005). Auxetic behaviour from **rotating rigid** units. Physica Status Solidi (B), 242(3), 561–575.

Grima, J. N., Chetcuti, E., Manicaro, E., Attard, D., Camilleri, M., Gatt, R., & Evans, K. E. (2011). On the auxetic properties of generic **rotating rigid triangles**. Proceedings of the Royal Society A: Mathematical, Physical and Engineering Sciences, 468(2139), 810–830.

Grima, J., Zammit, V., Gatt, R., Alderson, A., & Evans, K. (2007). Auxetic behaviour from rotating **semi-rigid units**. Physica Status Solidi (B), 244(3), 866–882.

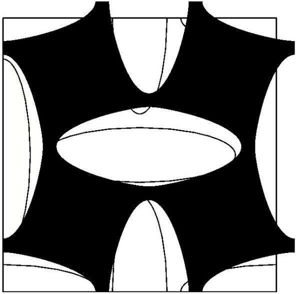

Our result from 2010

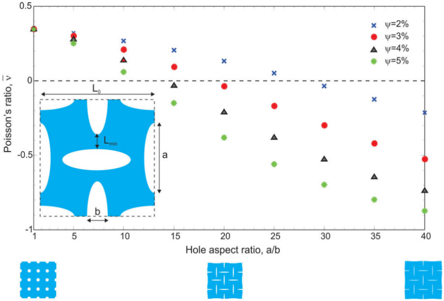

Taylor, M., Francesconi, L., Gerendás, M., Shanian, A., Carson, C., & Bertoldi, K. (2014). Advanced Materials, **26**(15), 2365–70.

Motivation – rotating units

Grima, J. N., Alderson, A., & Evans, K. E. (2005). Auxetic behaviour from **rotating rigid** units. Physica Status Solidi (B), 242(3), 561–575.
Grima, J. N., Chetcuti, E., Manicaro, E., Attard, D., Camilleri, M., Gatt, R., & Evans, K. E. (2011). On the auxetic properties of generic **rotating rigid triangles**. Proceedings of the Royal Society A: Mathematical, Physical and Engineering Sciences, 468(2139), 810–830.
Grima, J., Zammit, V., Gatt, R., Alderson, A., & Evans, K. (2007). Auxetic behaviour from rotating **semi-rigid units**. Physica Status Solidi (B), 244(3), 866–882.

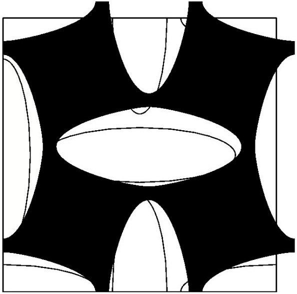

Our result from 2010

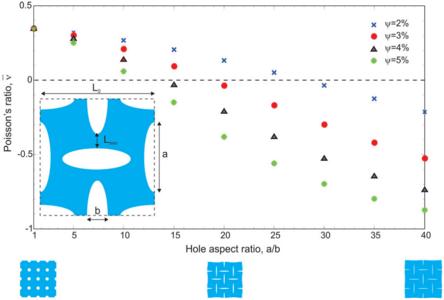

Taylor, M., Francesconi, L., Gerendás, M., Shanian, A., Carson, C., & Bertoldi, K. (2014). Advanced Materials, **26**(15), 2365–70.

Why not fill the gaps?

Structures

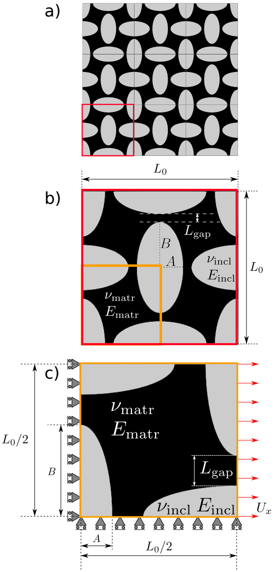

Geometry:

- Periodically arranged ellipses
- Alternating axes (perpendicular)

Repeating unit cell (RUC):

- 4 rotating units
- Periodic mesh

Boundary conditions within **reduced RUC**

- All boundaries remain straight lines
- Less computational resources needed

Simulations – Finite Elements

1. Abaqus/CAE via Python interface generates `inp` files (`wc -l ellipses-uniform-mesh.py` gives 640 lines),
2. Abaqus/STANDARD performs simulations generating `odb` files,
3. Abaqus/CAE extracts important information from each `odb` file.

One run is enough to calculate ν as well as E in one direction:

$$\nu_{\text{eff}} = -\frac{V_y / H_0}{U_x / W_0}. \tag{1}$$

$$E_{\text{eff}} = \frac{2 \; E^{\text{elas}} \; W_0}{T \; U_x^2 \; H_0}. \tag{2}$$

- V_y the displacement of (an arbitrary) top node
- E^{elas} elastic deformation energy
- T denotes the plane-stress thickness.
- U_x known deformation

Meshes: uniform vs. non-uniform

The discretization (meshing) is an essential and most challenging step on FE analysis.

Meshes: uniform vs. non-uniform

The discretization (meshing) is an essential and most challenging step on FE analysis.

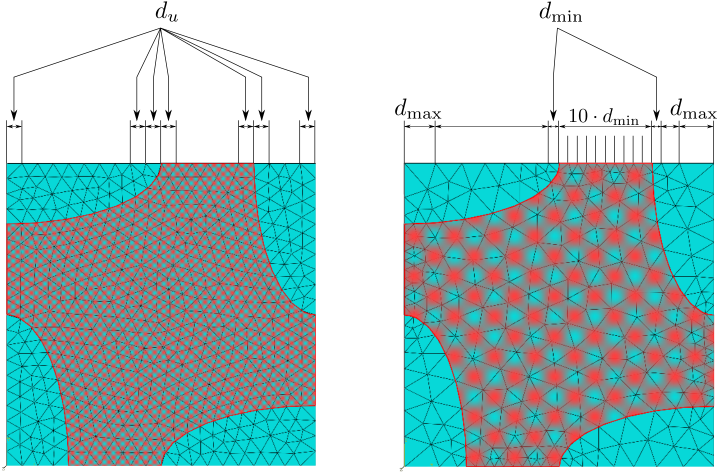

Mesh & convergence

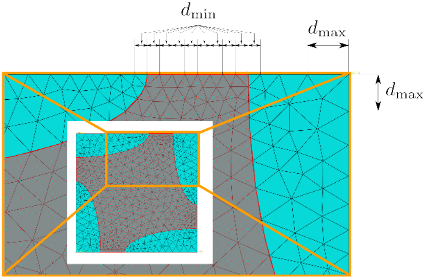

Figure: Nonuniform exemplary mesh. Each edge was assigned a bias seed in order to obtain possibly dense mesh in the narrowest (bottleneck) regions. In this case $L_{\text{gap}}/d_{\min} = 8$ was chosen in order to make he figure readable. In the simulations this ratio was 100. Fig. on the right shows that the convergence tests were performed up to the value $d_{\min} = 10^{-4}$

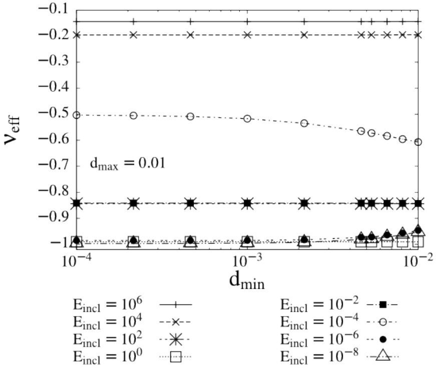

Figure: Convergence of Poisson's ratio as a function of $d_{\min}$ at fixed $d_{\max} = 0.01$. Here $\nu_{\text{matr}} = \nu_{\text{incl}} = -0.99$, $E_{\text{matr}} = 1$. The geometric parameters are: $a = 0.09$, $b = 0.89$. The convergence displays various characteristics depending on the value of E_{incl}.

Mesh & convergence

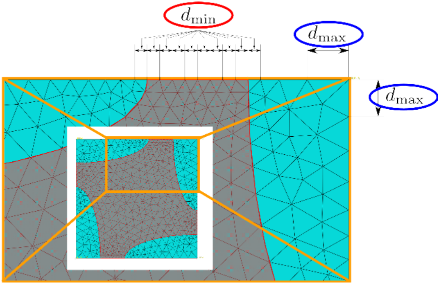

Figure: Nonuniform exemplary mesh. Each edge was assigned a bias seed in order to obtain possibly dense mesh in the narrowest (bottleneck) regions. In this case $L_{gap}/d_{min} = 8$ was chosen in order to make he figure readable. In the simulations this ratio was 100. Fig. on the right shows that the convergence tests were performed up to the value $d_{min} = 10^{-4}$

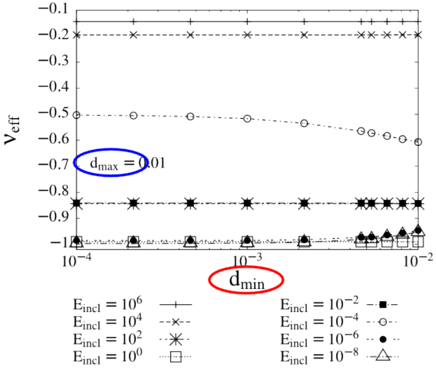

Figure: Convergence of Poisson's ratio as a function of d_{min} at fixed $d_{max} = 0.01$. Here $\nu_{matr} = \nu_{incl} = -0.99$, $E_{matr} = 1$. The geometric parameters are: $a = 0.09$, $b = 0.89$. The convergence displays various characteristics depending on the value of E_{incl}.

Convergence

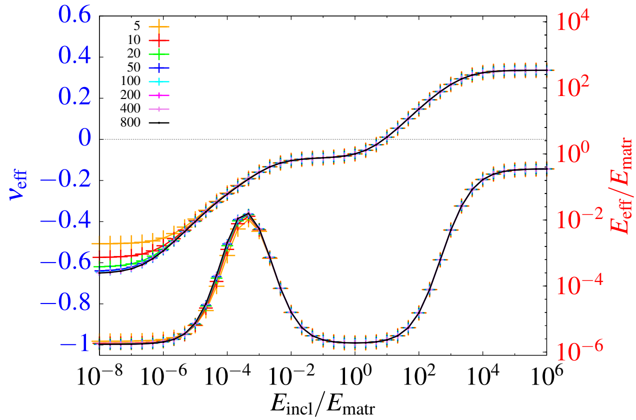

Figure: Convergence of $\nu_{\rm eff}$ and $E_{\rm eff}/E_{\rm matr}$ as obtained within **non-uniform meshing** for $a = 0.09$, $b = 0.89$, $\nu_{\rm incl} = \nu_{\rm matr} = -0.99$ and **increasing mesh density**. The upper, monotonic curves refer to the right (Young's modulus, red) axis, while the non monotonic curves refer to the left (Poisson's ratio, blue) axis. The numbers in the legend stand for the $L_{\rm gap}/d_{\rm min}$ ratio.

Detailed convergence – ν

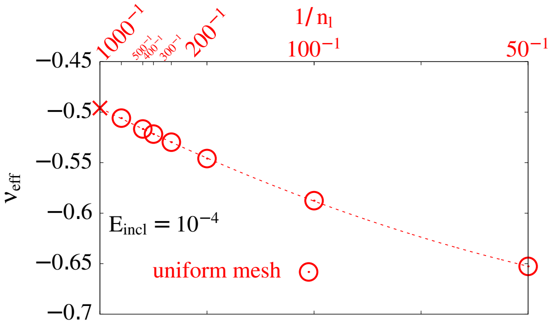

Detailed convergence – ν

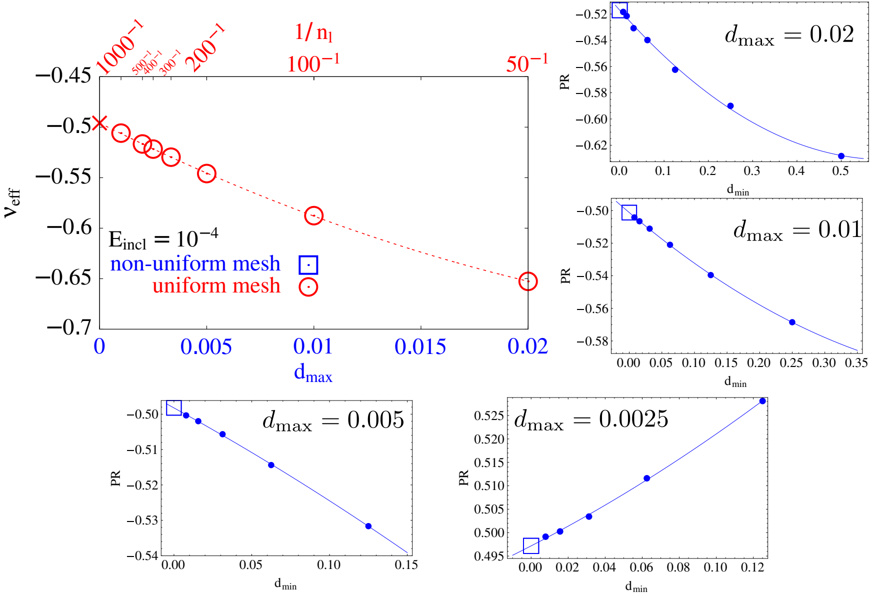

Detailed convergence – ν

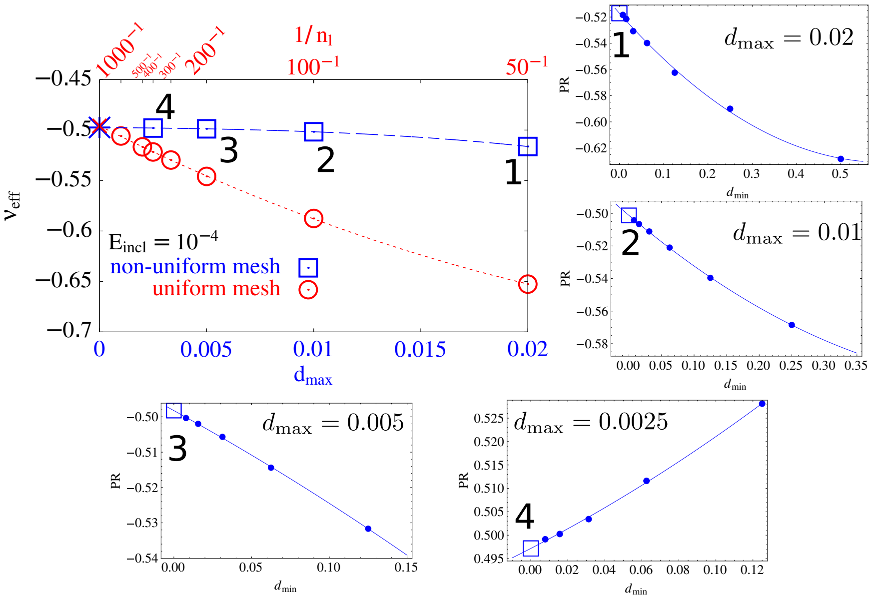

Detailed convergence – E

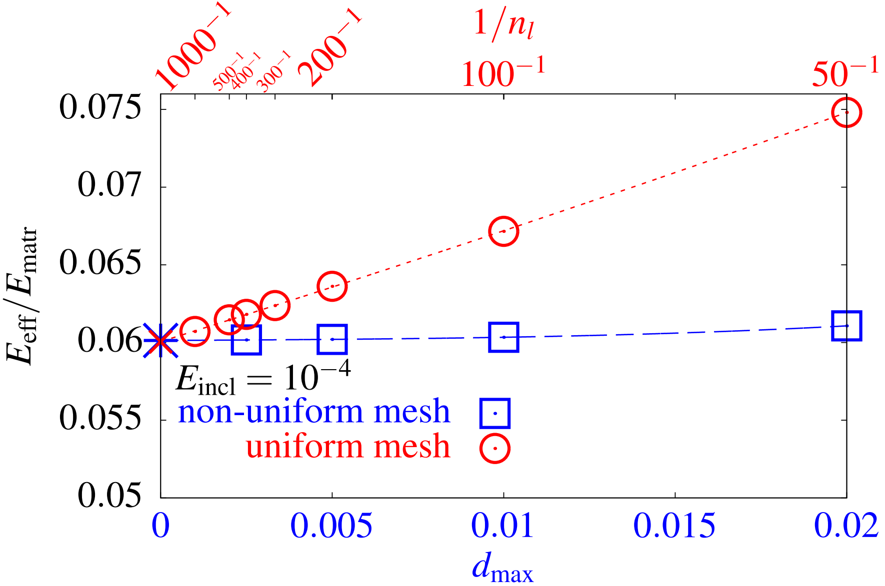

Required time vs. nuber of FE layers

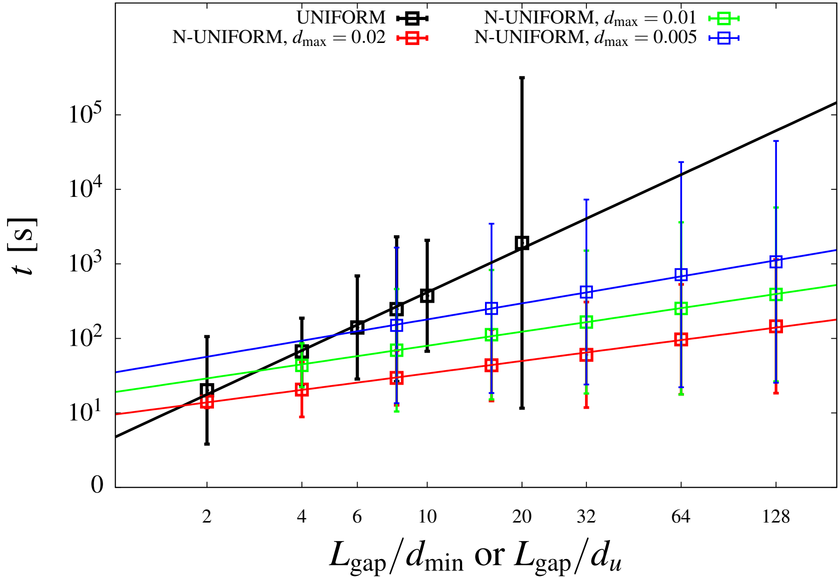

Memory consumed vs. nuber of FE layers

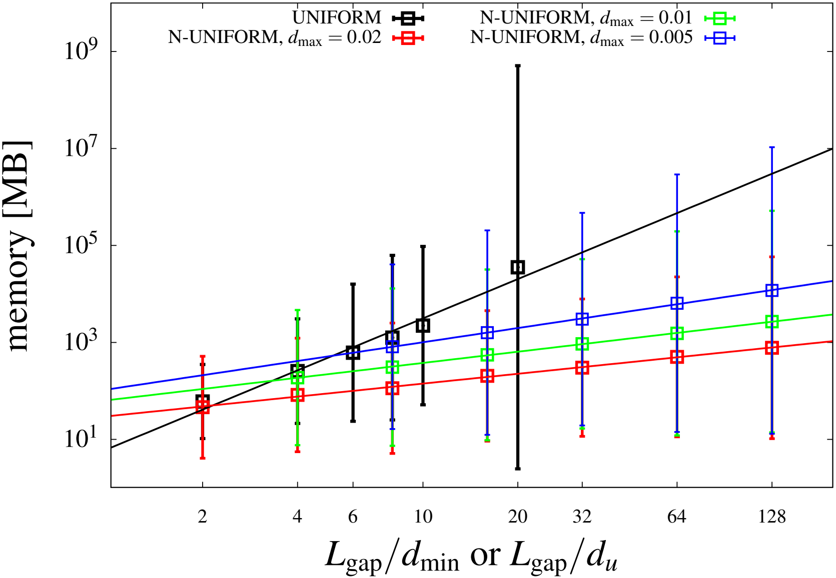

Results

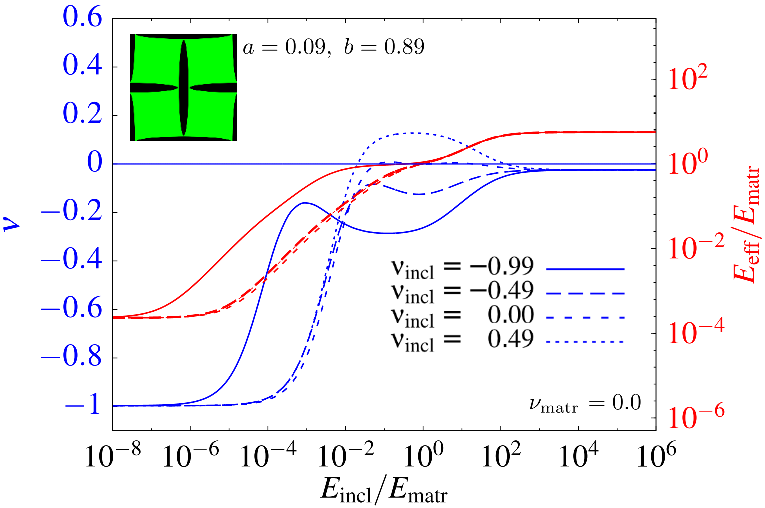

$a = 0.09, \ b = 0.89$
ν
$E_{\mathrm{eff}}/E_{\mathrm{matr}}$
$E_{\mathrm{incl}}/E_{\mathrm{matr}}$
$\nu_{\mathrm{incl}} = -0.99$
$\nu_{\mathrm{incl}} = -0.49$
$\nu_{\mathrm{incl}} = 0.00$
$\nu_{\mathrm{incl}} = 0.49$
$\nu_{\mathrm{matr}} = 0.0$
0.6 0.4 0.2 0 −0.2 −0.4 −0.6 −0.8 −1
10^{2} 10^{0} 10^{-2} 10^{-4} 10^{-6}
10^{-8} 10^{-6} 10^{-4} 10^{-2} 10^{0} 10^{2} 10^{4} 10^{6}

Results

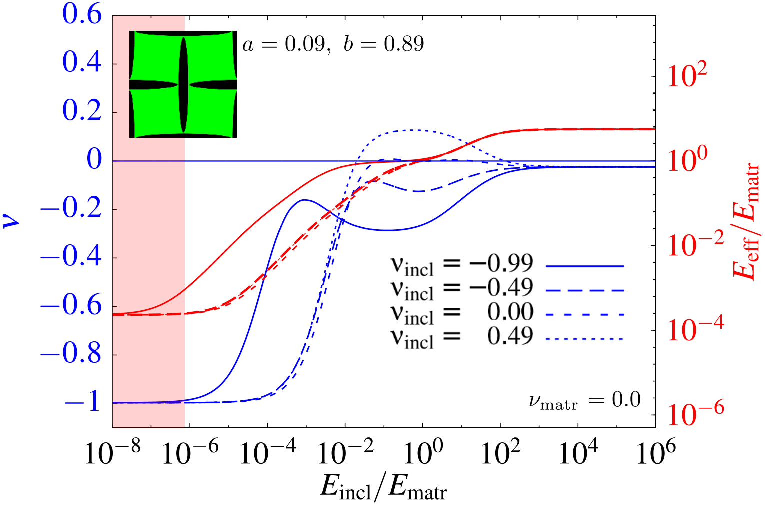

$a = 0.09, \; b = 0.89$
0.6
0.4
0.2
0
−0.2
−0.4
−0.6
−0.8
−1
ν
10^2
10^0
10^{-2}
10^{-4}
10^{-6}
$E_{\mathrm{eff}}/E_{\mathrm{matr}}$
$\nu_{\mathrm{incl}} = -0.99$
$\nu_{\mathrm{incl}} = -0.49$
$\nu_{\mathrm{incl}} = 0.00$
$\nu_{\mathrm{incl}} = 0.49$
$\nu_{\mathrm{matr}} = 0.0$
10^{-8} 10^{-6} 10^{-4} 10^{-2} 10^0 10^2 10^4 10^6
$E_{\mathrm{incl}}/E_{\mathrm{matr}}$

Results

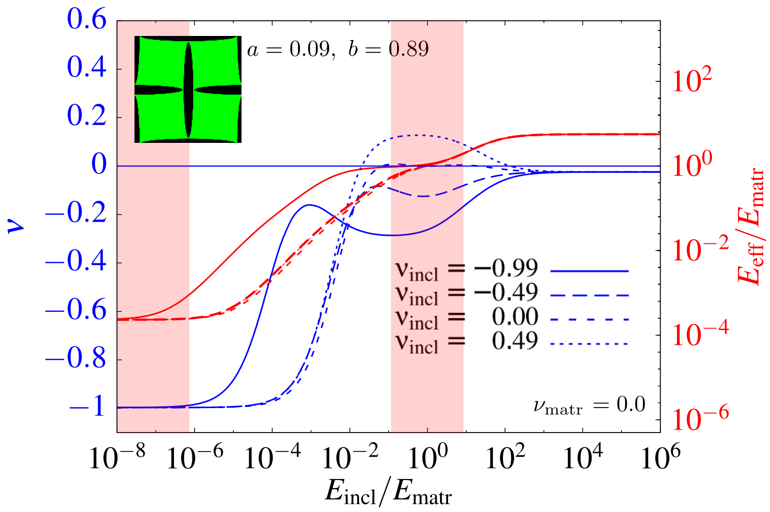

$a = 0.09, \; b = 0.89$
0.6
0.4
0.2
0
−0.2
−0.4
−0.6
−0.8
−1
ν
10^{2}
10^{0}
10^{-2}
10^{-4}
10^{-6}
$E_{\mathrm{eff}}/E_{\mathrm{matr}}$
$\nu_{\mathrm{incl}} = -0.99$
$\nu_{\mathrm{incl}} = -0.49$
$\nu_{\mathrm{incl}} = 0.00$
$\nu_{\mathrm{incl}} = 0.49$
$\nu_{\mathrm{matr}} = 0.0$
10^{-8} 10^{-6} 10^{-4} 10^{-2} 10^{0} 10^{2} 10^{4} 10^{6}
$E_{\mathrm{incl}}/E_{\mathrm{matr}}$

Results

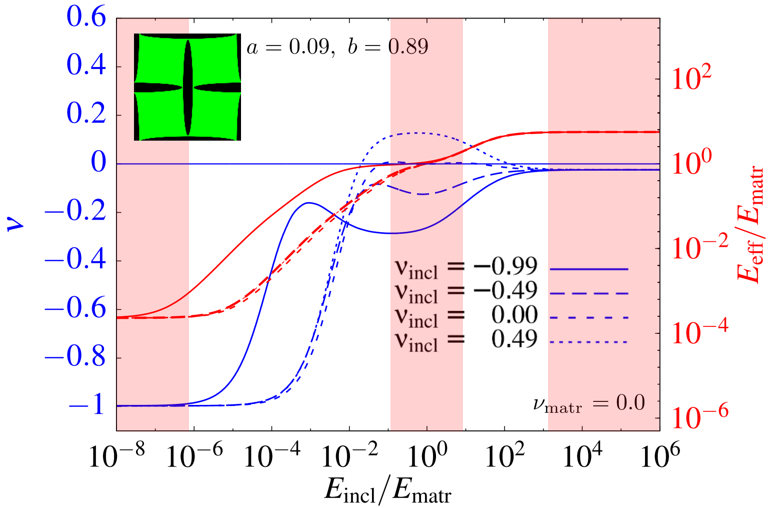

$a = 0.09,\ b = 0.89$
0.6
0.4
0.2
0
−0.2
−0.4
−0.6
−0.8
−1
ν
10^2
10^0
10^{-2}
10^{-4}
10^{-6}
$E_{\rm eff}/E_{\rm matr}$
$\nu_{\rm incl} = -0.99$
$\nu_{\rm incl} = -0.49$
$\nu_{\rm incl} = 0.00$
$\nu_{\rm incl} = 0.49$
$\nu_{\rm matr} = 0.0$
10^{-8} 10^{-6} 10^{-4} 10^{-2} 10^0 10^2 10^4 10^6
$E_{\rm incl}/E_{\rm matr}$

Results

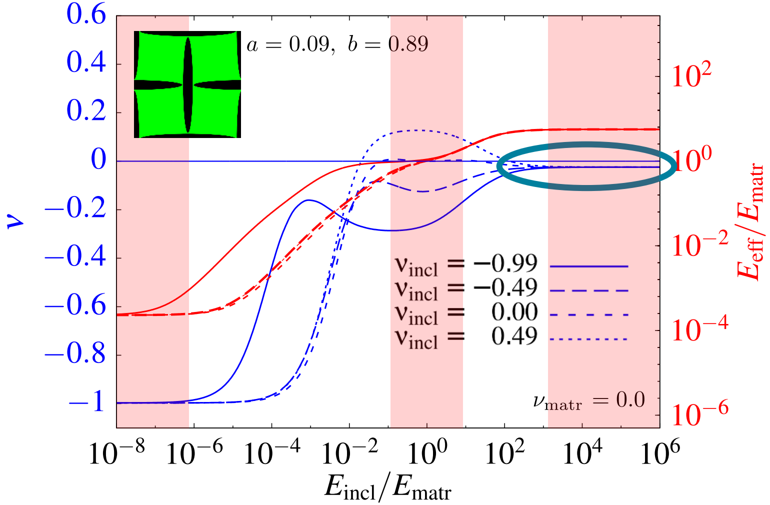

$a = 0.09,\ b = 0.89$
0.6
0.4
0.2
0
−0.2
−0.4
−0.6
−0.8
−1
ν
10^{2}
10^{0}
10^{-2}
10^{-4}
10^{-6}
$E_{\mathrm{eff}}/E_{\mathrm{matr}}$
$\nu_{\mathrm{incl}} = -0.99$
$\nu_{\mathrm{incl}} = -0.49$
$\nu_{\mathrm{incl}} = 0.00$
$\nu_{\mathrm{incl}} = 0.49$
$\nu_{\mathrm{matr}} = 0.0$
10^{-8} 10^{-6} 10^{-4} 10^{-2} 10^{0} 10^{2} 10^{4} 10^{6}
$E_{\mathrm{incl}}/E_{\mathrm{matr}}$

Results

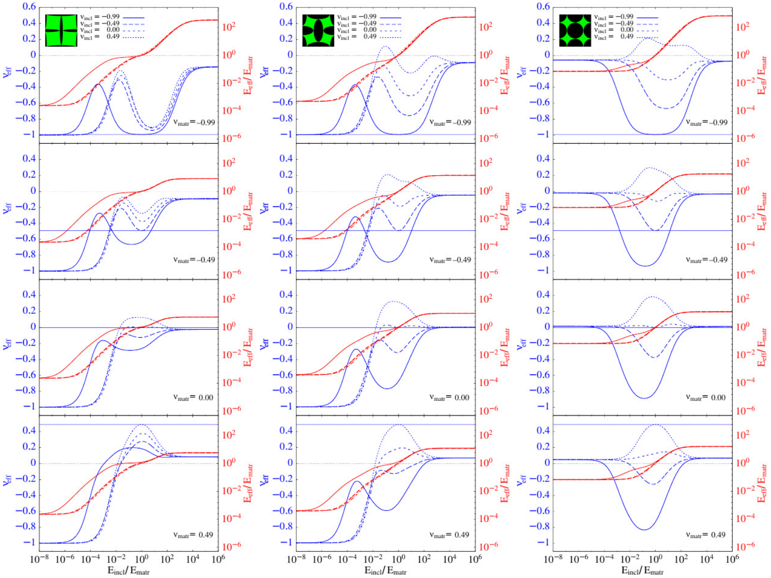

(a) $a = 0.09,\ b = 0.89$ (b) $a = 0.29,\ b = 0.69$ (c) $a = 0.49,\ b = 0.49$

E_{incl} limits, anisotropy

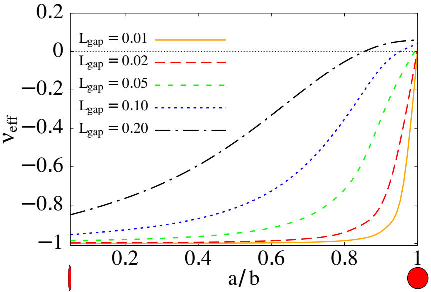

Void limit, $E_{\text{incl}} \to 0$

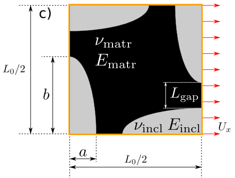

The dependence of Poisson's ratio as a function of a/b for various values of L_{gap}. Here both ν_{matr} and ν_{incl} are equal 0.

E_{incl} limits, anisotropy

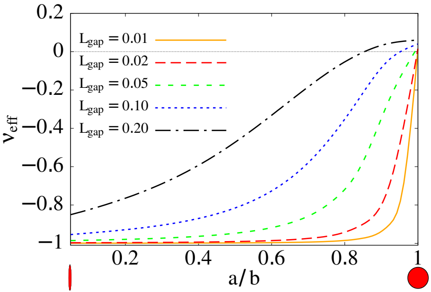

Void limit, $E_{\mathrm{incl}} \to 0$

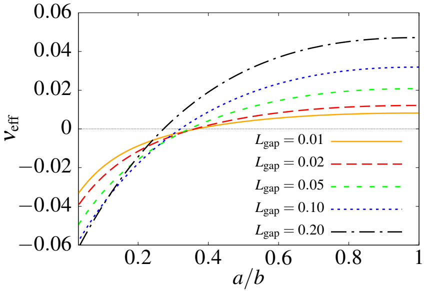

Rigid limit, $E_{\mathrm{incl}} \to \infty$

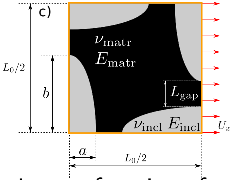

The dependence of Poisson's ratio as a function of a/b for various values of L_{gap}. Here both ν_{matr} and ν_{incl} are equal 0.

Rigid inclusions, $f(L_{\mathrm{gap}})$

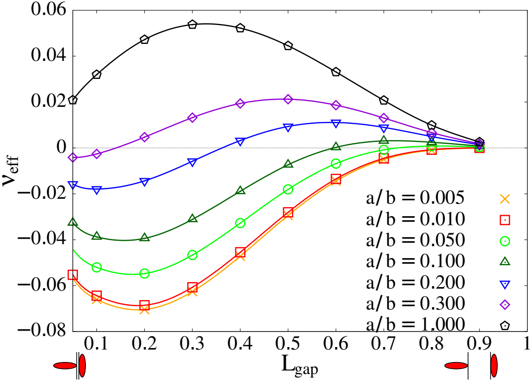

Figure: The dependence of Poisson's ratio as a function of L_{gap} for various values of a/b within the rigid inclusion limit. Here both ν_{matr} and ν_{incl} are equal 0.

Rigid inclusions, $f(\nu_{\mathrm{matr}})$

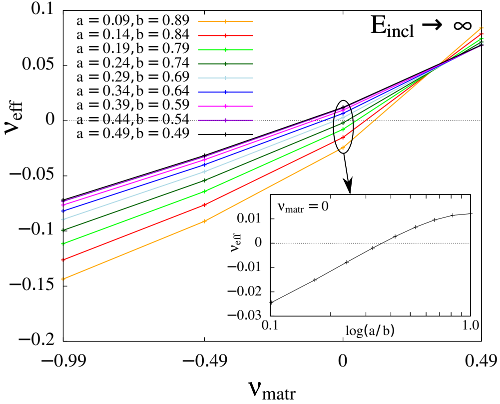

Figure: The dependence of effective Poisson's ratio as a function of the matrix Poisson's ratio in the limit of infinitely hard inclusions ($E_{\mathrm{incl}} \to \infty$). The value of ν_{incl} in this limit has no impact on the effective properties since the inclusions do not deform. The inset figure helps in estimating of the a/b ratio, for which ν_{eff} changes sign.

More and more auxetic constituents

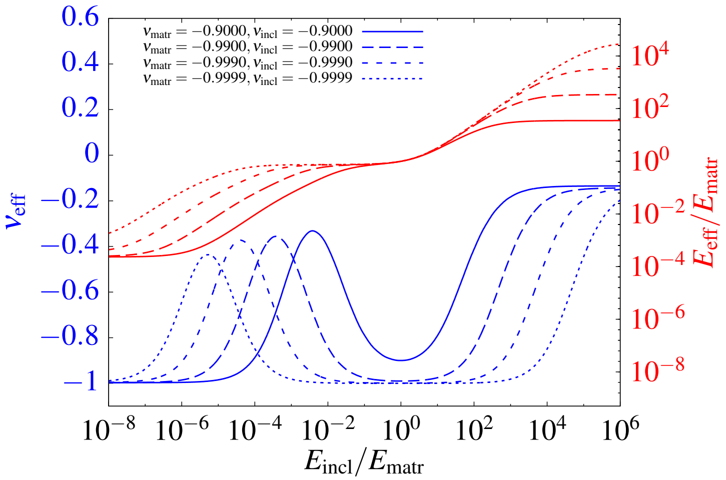

Figure: Effective Poisson's ratio, ν_{eff}, (blue colour) and effective Young's modulus, $E_{\mathrm{eff}}/E_{\mathrm{matr}}$, (red colour) as functions of $E_{\mathrm{incl}}/E_{\mathrm{matr}}$ for strongly auxetic matrices and inclusions.

Large deformations

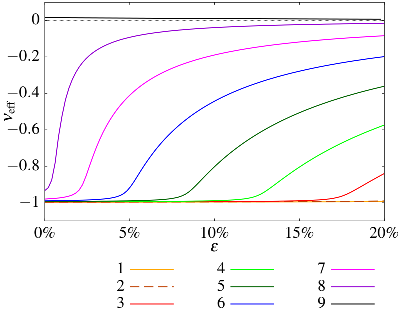

Poisson's ratio

Effective Poisson's ratio, ν_{eff}, and effective Young's modulus, $E_{\text{eff}}/E_{\text{matr}}$ as functions of nominal strain for $\nu_{\text{matr}} = 0$ and "void" inclusions (the material of inclusions is entirely removed). The numbers in the legend correspond to the following geometry parameter pairs: 1) $a = 0.09,\ 0.89$, 2) $a = 0.14,\ 0.84$, 3) $a = 0.19,\ 0.79$, 4) $a = 0.24,\ 0.74$, 5) $a = 0.29,\ 0.69$, 6) $a = 0.34,\ 0.64$, 7) $a = 0.39,\ 0.59$, 8) $a = 0.44,\ 0.54$, 9) $a = 0.49,\ 0.49$.

Large deformations

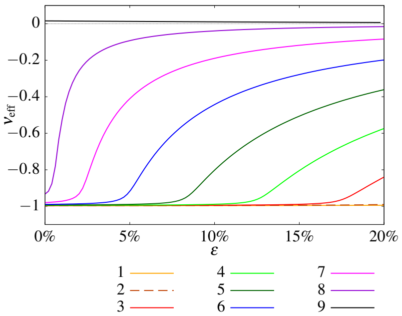

Poisson's ratio

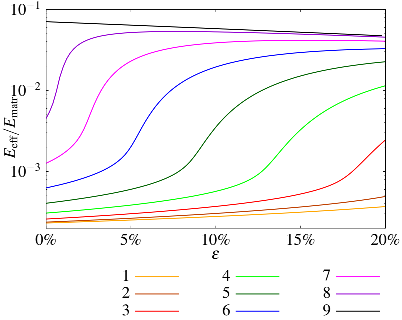

Young's modulus

Effective Poisson's ratio, ν_{eff}, and effective Young's modulus, $E_{\mathrm{eff}}/E_{\mathrm{matr}}$ as functions of nominal strain for $\nu_{\mathrm{matr}} = 0$ and "void" inclusions (the material of inclusions is entirely removed). The numbers in the legend correspond to the following geometry parameter pairs: 1) $a = 0.09,\ 0.89$, 2) $a = 0.14,\ 0.84$, 3) $a = 0.19,\ 0.79$, 4) $a = 0.24,\ 0.74$, 5) $a = 0.29,\ 0.69$, 6) $a = 0.34,\ 0.64$, 7) $a = 0.39,\ 0.59$, 8) $a = 0.44,\ 0.54$, 9) $a = 0.49,\ 0.49$.

Star-like inclusions, parameters a and b

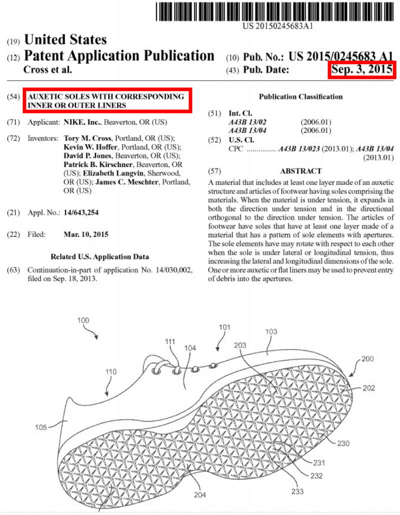

US 20150245683A1

(19) **United States**
(12) **Patent Application Publication**
Cross et al.

(10) **Pub. No.: US 2015/0245683 A1**
(43) **Pub. Date: Sep. 3, 2015**

(54) AUXETIC SOLES WITH CORRESPONDING INNER OR OUTER LINERS

(71) Applicant: **NIKE, Inc.**, Beaverton, OR (US)

(72) Inventors: **Tory M. Cross**, Portland, OR (US); **Kevin W. Hoffer**, Portland, OR (US); **David P. Jones**, Beaverton, OR (US); **Patrick B. Kirschner**, Beaverton, OR (US); **Elizabeth Langvin**, Sherwood, OR (US); **James C. Meschter**, Portland, OR (US)

(21) Appl. No.: **14/643,254**

(22) Filed: **Mar. 10, 2015**

Related U.S. Application Data

(63) Continuation-in-part of application No. 14/030,002, filed on Sep. 18, 2013.

Publication Classification

(51) **Int. Cl.**
A43B 13/02 (2006.01)
A43B 13/04 (2006.01)

(52) **U.S. Cl.**
CPC *A43B 13/023* (2013.01); *A43B 13/04* (2013.01)

(57) **ABSTRACT**

A material that includes at least one layer made of an auxetic structure and articles of footwear having soles comprising the materials. When the material is under tension, it expands in both the direction under tension and in the directional orthogonal to the direction under tension. The articles of footwear have soles that have at least one layer made of a material that has a pattern of sole elements with apertures. The sole elements have may rotate with respect to each other when the sole is under lateral or longitudinal tension, thus increasing the lateral and longitudinal dimensions of the sole. One or more auxetic or flat liners may be used to prevent entry of debris into the apertures.

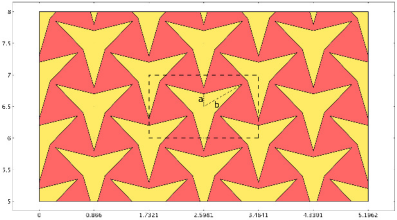

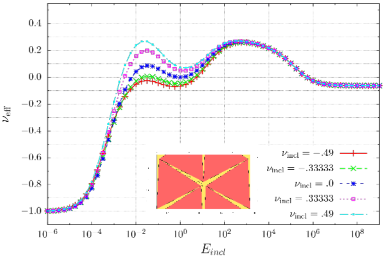

$$a = 0.05, \;\; b = 0.945$$

Star-like inclusions, parameters a and b

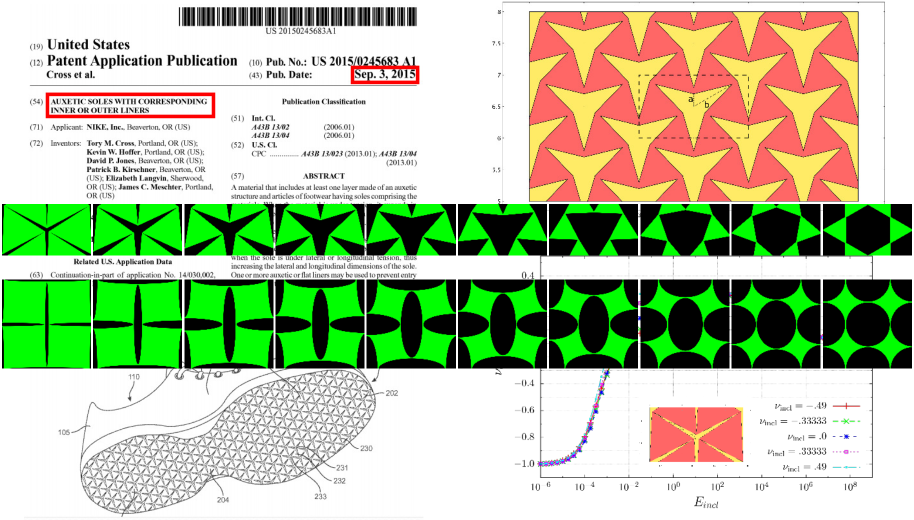

$$a = 0.05, \;\; b = 0.945$$

Conclusions

- For strongly anisotropic inclusions the effective Poisson's ratio, which is close to -1 for very low $E_\mathrm{incl}/E_\mathrm{matr}$, **grows** and after reaching a maximum (of negative value) **decays** to the matrix values close to $E_\mathrm{incl}/E_\mathrm{matr} \approx 1$ and then **grows** again to the large $E_\mathrm{incl}/E_\mathrm{matr}$ limit.

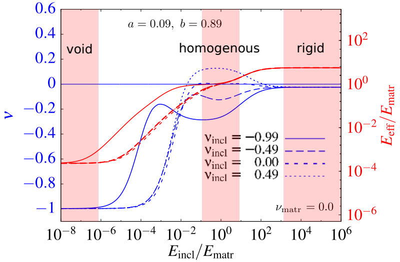

Conclusions

- For strongly anisotropic inclusions the effective Poisson's ratio, which is close to -1 for very low $E_{\mathrm{incl}}/E_{\mathrm{matr}}$, **grows** and after reaching a maximum (of negative value) **decays** to the matrix values close to $E_{\mathrm{incl}}/E_{\mathrm{matr}} \approx 1$ and then **grows** again to the large $E_{\mathrm{incl}}/E_{\mathrm{matr}}$ limit.
- In the vicinity of $E_{\mathrm{incl}}/E_{\mathrm{matr}}$ for which the effective PR shows its maximum, for the most auxetic inclusions the **effective Young's modulus is essentially larger** than for less auxetic inclusions.

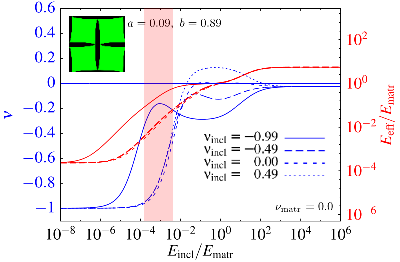

Conclusions

- For strongly anisotropic inclusions the effective Poisson's ratio, which is close to -1 for very low $E_{\rm incl}/E_{\rm matr}$, **grows** and after reaching a maximum (of negative value) **decays** to the matrix values close to $E_{\rm incl}/E_{\rm matr} \approx 1$ and then **grows** again to the large $E_{\rm incl}/E_{\rm matr}$ limit.
- In the vicinity of $E_{\rm incl}/E_{\rm matr}$ for which the effective PR shows its maximum, for the most auxetic inclusions the **effective Young's modulus is essentially larger** than for less auxetic inclusions.
- For highly anisotropic inclusions of very large Young's modulus, the effective PR of the composite can be **negative** for **nonauxetic** matrix and inclusions. These is a very simple example of an auxetic structure being not only **entirely continuous**, i.e. without empty regions (cuts, holes) introduced into the system, but with $E_{\rm incl} \gg E_{\rm matr}$, i.e. **inclusions (much) harder than the matrix**.

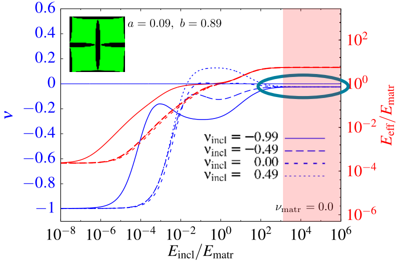

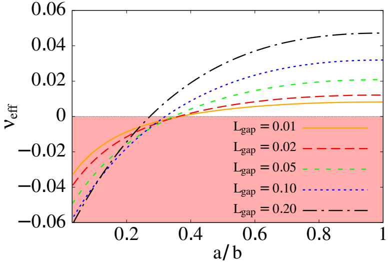

The end

Thank you for your attention

This work was supported by the (Polish) National Centre for Science under the grant NCN 2012/05/N/ST5/01476.

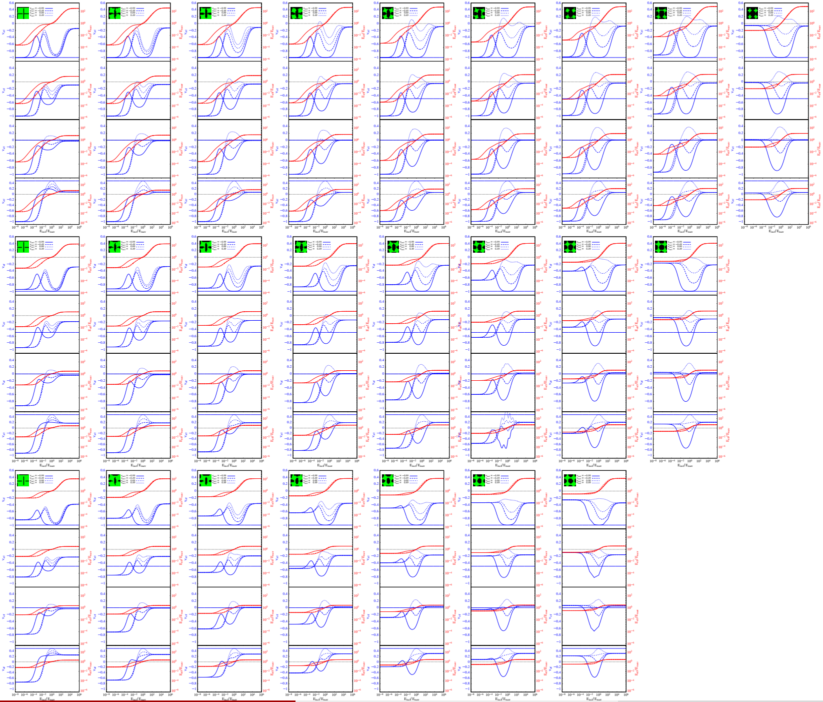

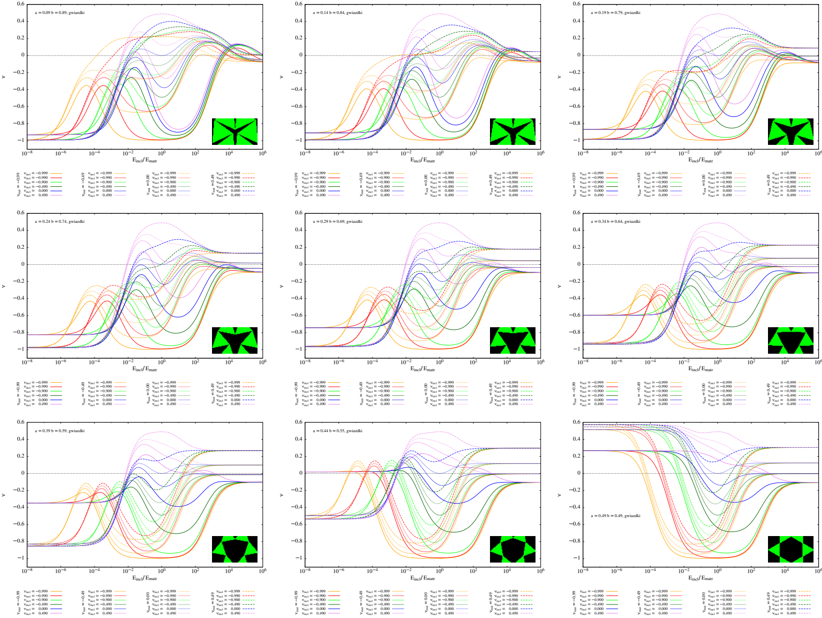
a = 0.09 b = 0.89, gwiazdki
a = 0.14 b = 0.84, gwiazdki
a = 0.19 b = 0.79, gwiazdki
a = 0.24 b = 0.74, gwiazdki
a = 0.29 b = 0.69, gwiazdki
a = 0.34 b = 0.64, gwiazdki
a = 0.39 b = 0.59, gwiazdki
a = 0.44 b = 0.55, gwiazdki
a = 0.49 b = 0.49, gwiazdki
ν
E_{incl}/E_{matr}